



Alteration in Lactate Production and Decrease in MTT Dye Reduction in Serum-starved Human Peripheral Blood Mononuclear Cells (PBMCs)

Maryam Mehri¹, Fatemeh Saeedi¹, Roghayeh Porbagher² and Amrollah Mastafazadeh^{2,*}

¹Students Research Committee, Babol University of Medical Sciences, Babol, Iran

²Cellular and Molecular Biology Research Center, Health Research Institute, Babol University of Medical Sciences, Babol, Iran

*Corresponding author: Cellular and Molecular Biology Research Center, Health Research Institute, Babol University of Medical Sciences, Babol, Iran. Email: amrolah65@gmail.com

Received 2021 May 05; Revised 2021 May 13; Accepted 2021 May 13.

Abstract

Background: Immunometabolism targeting therapy of auto-inflammatory diseases is an emerging strategy compared to immune system global suppression. However, our knowledge in this field needs promotion.

Objectives: We examined the effects of serum starvation stress on metabolic activity in human peripheral blood mononuclear cells (PBMCs).

Methods: Fresh immune cells were isolated from four healthy adult volunteers and cultivated with or without fetal bovine serum (FBS) at various time points under standard conditions. Glucose and intra- and extracellular lactate levels were assessed using routine techniques, and 3-(4, 5 -dimethylthiazol-2-yl)-2, 5-diphenyl tetrazolium bromide (MTT) reduction assay was used to determine mitochondrial function.

Results: Spindle shape macrophage-like cells, which appeared early, were replaced at 96 h by large round monocytes/macrophage-like cells, with more frequency in the non-starved group. Interestingly, serum starvation dictated a status, especially in monocyte/macrophage-like cells, that led to prolong decrement in mitochondrial dehydrogenase-mediated reduction of MTT. This difference was confirmed with the MTT assay quantitatively ($P < 0.05$). Moreover, the intra- and extracellular lactate concentrations were lower in starved cells than in non-starved controls ($P < 0.05$), and glucose levels were higher in 72 h starved cell culture supernatants than in non-starved control cells ($P < 0.05$).

Conclusions: This study showed that under serum starvation-induced metabolic stress, lactate production is altered in immune cells, and total oxidative mitochondrial activity is reduced in macrophage-like cells. These findings open a new window to target immune cell metabolism for the treatment of autoinflammatory and autoimmune diseases.

Keywords: Metabolism, Serum, Lactate, Immune System, COVID-19

1. Background

Cell metabolism plays a key role in immune cells' biology. Like in other cells, metabolism enables the immune cells to perform intricately and efficiently their multi-facet functions such as homeostasis, defense against different pathogenic germs, and protection against a variety of cancerous cells. These tasks collectively grant human life in this hostile world. Growth factors and nutrients such as glucose and amino acids are the main players in cell metabolism. Glucose is an aldohexose that is available for most cells, including immune cells through blood circulation and then through special transporters located in cell membranes called GLUT. For instance, the activated hu-

man T-lymphocyte expresses GLUT1, not GLUT4 (1). After entering the cells, glucose changes to pyruvic acid through the pathway of glycolysis, which, in turn, is converted to lactate if oxygen is not available; this occurs, for instance, in neutrophils that combat pyogenic bacteria under pus circumstances (2). Surprisingly, sometimes, despite oxygen availability, some dividing cells like cancerous cells and immune cells enhance glycolysis, which is called aerobic glycolysis in those conditions (Warburg effect) (3), described first by Otto Warburg in 1923 (4). On the other hand, pyruvic acid may undergo some biochemical changes to produce nicotinamide adenine dinucleotide phosphate (NADPH₂) in mitochondria through the Krebs

cycle. The presence of this molecule with the redox property forms the basis of the MTT assay in the estimation of cell viability and cell count (5).

Amino acids exhibit two fundamental roles in cell biology. On the one hand, as building blocks of protein molecules, these acids contribute to protein synthesis in ribosomes, and subsequently, different types of proteins are involved in cell survival and growth. There are 21 amino acids in the cells. If one of these amino acids is not available, the general protein synthesis will be shut down in the cells, and then, the special type of protein synthesis will be triggered, mediating the integrated stress response (ISR) to support cell survival under such metabolic stress conditions (6). On the other hand, in cooperation with growth factors such as insulin or insulin-like growth factor, amino acids orchestrate some signaling pathways leading to the activation of one of the most important enzymes in cell metabolism, cell survival, and growth, i.e., mammalian target of rapamycin tyrosine kinase, a serin-threonine kinase with 289 kDa molecular weight (7). In the absence of such growth factors, mTOR activity will be sharply reduced, and subsequently, the generation of ribosomes, protein synthesis, and lipogenesis will be reduced, and cell metabolism is converted to an autophagy-based mechanism, which supports cell survival under growth factor deficiency stress conditions (8).

Autophagy can trigger apoptotic cell death program in a prolonged growth factor deficiency state, a phenomenon that can be recapitulated *in vitro* through serum starvation tools and cell culture techniques (9). Serum starvation is defined as a special cell culture condition in which the cells are cultivated in a cell culture medium containing glucose, amino acids, vitamins, and all other ingredients needed by cells for their metabolism, except animal/human serum. The serum may be absent or reduced to 1-to2% in the cell culture system (10). This type of metabolic stress may occur in some physiologic and pathologic conditions such as inflammation and cancers (11). Immune cells, in cooperation with other stromal cells like fibroblasts, must work in such circumstances to perform their homeostatic and protective activities. Thus, the *in vitro* study of those cells' behaviors under conditions of serum starvation may provide some data to estimate mechanisms used by those cells in their real combating niche with pathogenic germs and cancerous cells or the regulation of inflammatory reactions in autoinflammatory diseases like atherosclerosis, multiple sclerosis, and recently emerged Coronavirus Disease (COVID)-19 with overt hyperinflam-

mation manifestations (12).

In our previous study with human skin fibroblasts, we showed that in response to serum starvation stress, those cells produced a dozen of proteins with growth factor-like activity and with wound-healing potential (13). We recently reported that those starved fibroblasts-derived substances downregulated the stemness-related genes expression and induced necrosis in rat LA7 cancer stem cells and inhibited these cells' migration *in vitro* (14). We also showed that those substances downregulated Sox2, Nanog, and Oct4, and stemness-related genes in LA7-induced mammary gland tumors in rats and induced tumor necrosis in such experimental model of solid tumors (manuscript under review). Moreover, we already reported that in reaction to serum starvation stress, the human blood mononuclear cells (PBMCs) downregulated their surface human leukocyte antigen (HLA) class-I expression (15) and exhibited an enhanced level of immunoregulatory phenotype (16). We found an elevated level of lactate ions in starved human fibroblast culture, indicating a Warburg phenomenon induction by serum starvation in those cells. To our knowledge yet, there is no report about PBMCs' metabolic response to serum starvation.

2. Objectives

This research aimed to investigate the effects of serum starvation stress on the morphological and metabolic function of PBMCs.

3. Methods

3.1. Preparation of PBMCs

Five milliliters of whole blood were daily collected from each of the three healthy volunteers (all female, average age \pm standard deviation 26.00 ± 2.64 years) in heparinized sterile tubes for four consecutive days. Then, fresh PBMCs were isolated by Ficoll-Paque density-gradient centrifugation at 450 g for 30 min, and the viability percentage of the cells was determined by using the trypan blue dye exclusion test.

3.2. Serum Starvation and Serum Re-feeding Protocol

In a 24-well plate (SPL, Germany), about 0.5×10^6 fresh PBMCs ($n = 3$) were cultured in triplicate for 16, 48, 72, and 96 h in 800 μ L glucose-containing serum-free RPMI-1640 (Biowest, France) supplemented with 100 U/mL penicillin and 100 g/mL streptomycin (Sigma, Germany) in a

37°C incubator containing 5% CO₂. Moreover, in this plate as non-starved control cells, the same number of PBMCs was also cultured with the same volume of medium but supplemented with 10% fetal bovine serum (FBS) (Sigma, Germany). Then, the cells in each well were thoroughly resuspended and centrifuged (Sigma, 3K30, Germany) at 5,000 revolutions per minute (RPM) for five minutes at room temperature. Thereafter, the culture supernatant was harvested and stored at -20°C for further examination, as well as the cell pellet was washed with phosphate-buffered saline (PBS) through centrifugation as described above. The cell count was done by a Neubauer chamber, and the viability of the cells was determined using the trypan blue dye test. Moreover, in a separate experiment, another 23-year-old female volunteer was recruited, and 0.5×10^6 PBMCs were prepared from her and cultured for 16, 48, 72, and 96 h in glucose-containing serum-free RPMI-1640 with 100 U/mL penicillin and 100 g/mL streptomycin. The cells were also cultured as non-starved control in a complete medium supplemented with 100 U/mL penicillin, 100 g/mL streptomycin, and 10% Fetal Bovine Serum (FBS). The cultivation was carried out on a 24-well plate. Then, 16, 48, 72, and 96 h starved cells were collected for intracellular lactate analysis as described below.

For re-feeding experiments, the washed cells were dispensed to their related wells that had already been washed with PBS once. Then, both starved and non-starved cells were cultured in 10% FBS for another 96 h under standard cell culture conditions as described above. Finally, the MTT dye reduction test was performed based on the protocol described below.

3.3. MTT Dye Reduction Analysis

At the end of the serum re-feeding experiment, because PBMCs were cultured as a mixture of adherent and suspended cells, 200 µL of cell culture supernatant was replaced by 200 µL of MTT dye (5 mg/mL) (ACROS, New Jersey, USA) in each well. The plates were then slowly shaken and incubated at 37°C for four hours at 37°C under standard cell culture conditions as already described. Before dispensing 600 µL of dimethyl sulfoxide (DMSO) into each well, the extent of formazan crystals formation was thoroughly investigated at a single cell level in each well under an inverted microscope (Olympus, Germany), and the required microphotographs were captured by a camera equipped with GP25 software. Finally, the DMSO solubilized formazan was gently mixed, and 200 µL of this solution was transferred to a 96-well microtiter plate to deter-

mine the Optical Density (OD) at 570 for each well using a microplate reader (Rayto, China)

3.4. Lactate Measurement

The lactate levels in starved and non-starved PBMCs culture supernatants were determined using a routine clinical laboratory method, fluorometric lactate enzymatic assay (Biorexfars, Iran) Briefly, 10 µL of the specimen, RPMI medium only, RPMI medium + 10% FBS, and kit standard solution were mixed with 1 mL of kit reagent and incubated at 37°C for 10 min, and then, the OD of the test solution was obtained at 546 nm and compared with that of standard solution to calculate lactate concentrations according to the kit instruction. The data were expressed as mg/dL. The value obtained for the RPMI medium only- or RPMI medium + 10% FBS solution, was subtracted from the lactate concentrations of starved and non-starved cell culture supernatants to determine the amount of lactate produced by those cells. To determine the intracellular lactate levels, the cells were initially lysed by incubating at 100°C for 5 min and then cooled at room temperature. The kit sensitivity was 2 mg/dL.

3.5. Glucose Measurement

The glucose concentration was evaluated in starved and non-starved PBMCs culture supernatants using a Glucose GOD/PAP kit (Bionik, Iran). Based on the kit instruction, 10 µL of the test specimen or calibrator solution was mixed with 1 mL of kit reagent and incubated at 37°C for 10 min, and then, the OD of the test solution was obtained at 505 nm and compared with that of calibrator solution to calculate the glucose concentration. The data were expressed as mg/dL. The kit sensitivity was 1 mg/dL.

3.6. Statistical Analysis

The continuous data were presented as mean \pm standard deviation (SD). The Kolmogorov-Smirnov test was performed to determine the normality of the data. The mean values were compared using one-way ANOVA and Tukey's post hoc test or independent *t*-test for data with normal distribution. Otherwise, the Kruskal-Wallis and Mann-Whitney U tests were used. The graphs were drawn by GraphPad Prism 6.0. The data were analyzed by SPSS version 18 software (Chicago, USA) or Prism 6.0 program. A *P*-value < 0.05 was considered statistically significant in all statistical tests.

4. Results

4.1. Reduction in Cell Number and Morphological Changes in Serum-starved PBMCs

To evaluate the effects of serum starvation stress on morphological characteristics of cultured PBMCs, we observed thoroughly the adherent and non-adherent cell fractions under an inverted microscope. We also determined the cell number and viability to provide more details about cell survival under serum starvation conditions. We were not able to find a remarkable difference between lymphocytes in two groups morphologically even after 96 h. However, the most considerable finding in this regard was the cell aggregation formation, which predominantly appeared in non-starved cells just at 72 h time point whereas in starved cells such aggregation was observed scanty with much smaller size (Figure 1A panels e and f). In the adherent cell fraction, we found some spindle shape cells with more frequency in the non-starved group, which reached the maximum levels at 48 h of PBMCs culture (Figure 1A panels c and d). Those cells were replaced in the 96 h cultured cells by some large cells with granular cytoplasm albeit with much more frequency in the non-starved group. The cell count was not changed in the first 48 h of PBMCs culture under serum starvation metabolic stress, but this value reduced to a significant level in 72 h starved cells ($P < 0.01$). The reduction rate was enhanced in 96 h starved PBMCs ($P < 0.001$) (Figure 1B). However, we were not able to observe any dead cells in the trypan blue dye exclusion test.

4.2. Alterations in Glucose Concentrations and Lactate Accumulation in Starved and Non-starved Human PBMCs Culture Supernatants

To investigate the overall effects of serum starvation stress on glucose metabolisms, we measured the lactate and glucose levels in starved and non-starved PBMCs culture supernatants. We found that the total amount of lactate decreased in the starved group compared to non-starved cells significantly ($P < 0.0001$) at all indicated time points (Figure 2A). However, in both groups, the lactate levels in cell culture supernatants increased in a time-dependent manner ($P < 0.0001$). As Figure 2B shows, alterations in glucose concentrations of starved and non-starved PBMCs culture supernatants were not sharp. The difference in glucose concentrations between the two groups was significant only in 72 h cell incubation ($P < 0.05$).

4.3. Reduced Levels of Intracellular Lactate in Starved PBMCs

To evaluate the effects of serum starvation-induced metabolic stress on lactate production, we measured the intracellular levels of lactate in starved and non-starved immune cells. As can be seen in Figure 3, under serum starvation stress, the intracellular lactate levels significantly reduced in starved PBMCs versus non-starved cells with $P < 0.001$ and $P < 0.05$ at 16 h and 48 h time points, respectively.

4.4. Diminished Capacity of Starved PBMCs in MTT Dye Reduction

To investigate the prolonged effects of serum starvation-derived stress on cell survival and metabolism, we performed MTT reduction analysis after 96 h re-feeding with serum. Interestingly, the starved PBMCs exhibited a reduced level of formazan crystals formation at the single-cell level when thoroughly evaluated under an inverted microscope (Figure 4A and B). Our quantitative MTT assay data also confirmed this conclusion, which showed that this difference between starved and non-starved cells was statistically significant after 72 h of cell incubation ($P < 0.01$) (Figure 4C). In both groups, there was a remarkable fluctuation in cell capacity for MTT dye reduction. This capacity was increased in 48 h cultured cells when compared to 16 h incubated cells ($P < 0.05$ for both groups). Thereafter, compared with time point 48 h, this capacity was significantly decreased at time point 72 h (P -value < 0.05 in both groups). In starved and non-starved groups, this capacity returned to non-significant levels when compared with 48 h starved cells at time point 96 h. Our microscopic observations also showed that both starved cells and non-lymphocytes were not able to form visible purple formazan crystals in the MTT assay (Figure 4A).

5. Discussion

Our previous in vitro study showed that human PBMCs in response to serum starvation stress produce higher levels of an immune regulatory cytokine, i.e., Transforming Growth Factor (TGF)- β , and exhibit an elevated prevalence of CD4⁺ CD25⁺ CD127⁺ FOXP3⁺ T regulatory cells (16). However, we do not know the effect of serum starvation on PBMCs' general metabolism. In the present study, we evaluated the lactate level in serum-starved PBMCs as an end product of the glycolysis pathway compared to non-starved cell controls. We also compared the starved and non-starved cells based on the results derived from MTT dye

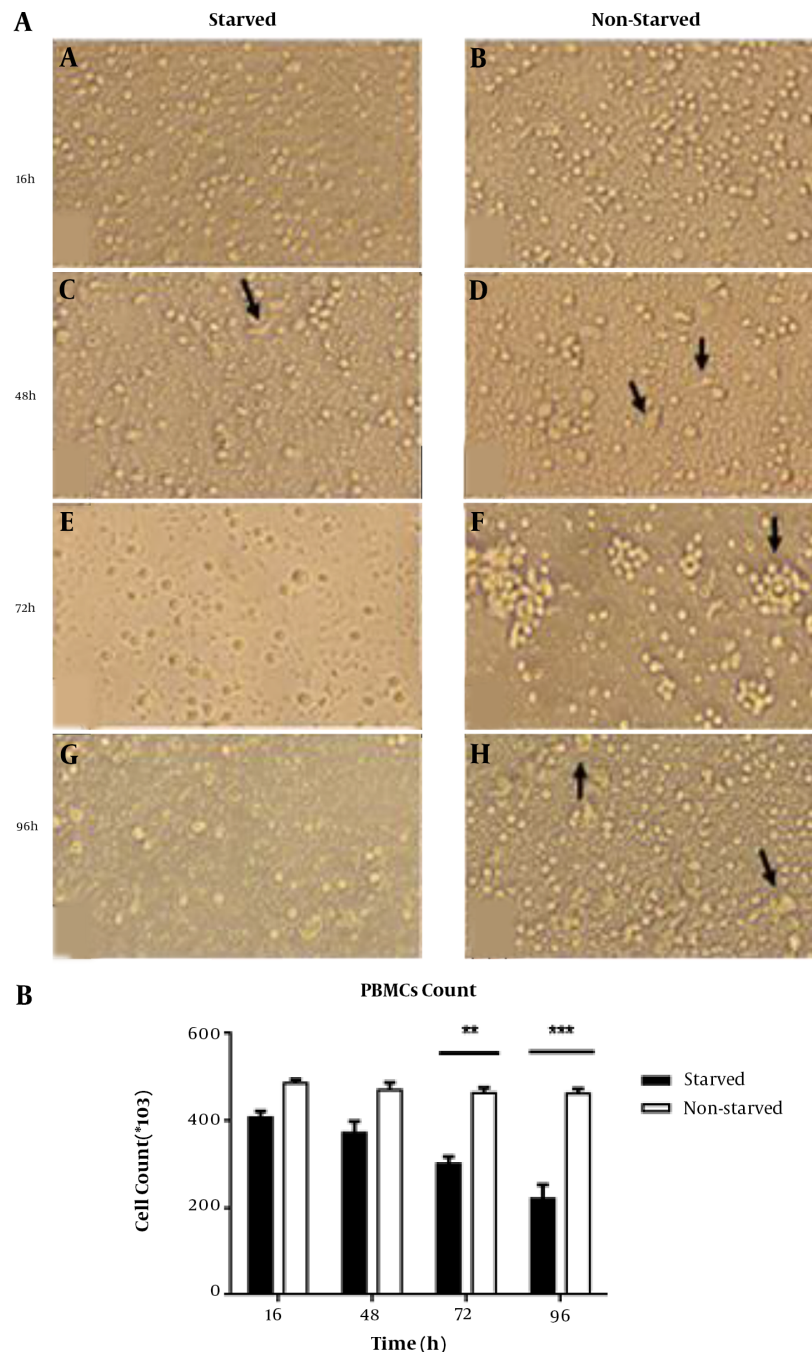


Figure 1. Morphological evaluation and cell count in starved and non-starved PBMCs. A, Cellular population and morphological changes in serum-starved and non-starved PBMCs. Invert microscopic image (20X) shows that after 16, 48, 72, and 96 h starvation, PBMCs were shiny (a, c, e, and g), but non-starved cells exhibited more- and larger-cell aggregation (arrow in panel f). At all time-points, spindle shape macrophage-like cells were observed, but in the 96 h starved and non-starved groups (g and h), these cells were replaced by large rounded cells with more prevalence in starved cells. B, The cell count of PBMCs in starvation and non-starvation conditions (n = 9; three samples with triplicate wells for each time point). The cell number was decreased gradually in the starved group and reached a significant difference compared to non-starved cells at 72 h time point ($P < 0.01$); at 96 h, this difference became more obvious ($P < 0.001$). Results are shown as mean \pm SD. The error bars indicate the standard deviation. ** $P < 0.01$ and *** $P < 0.001$ were considered statistically significant levels.

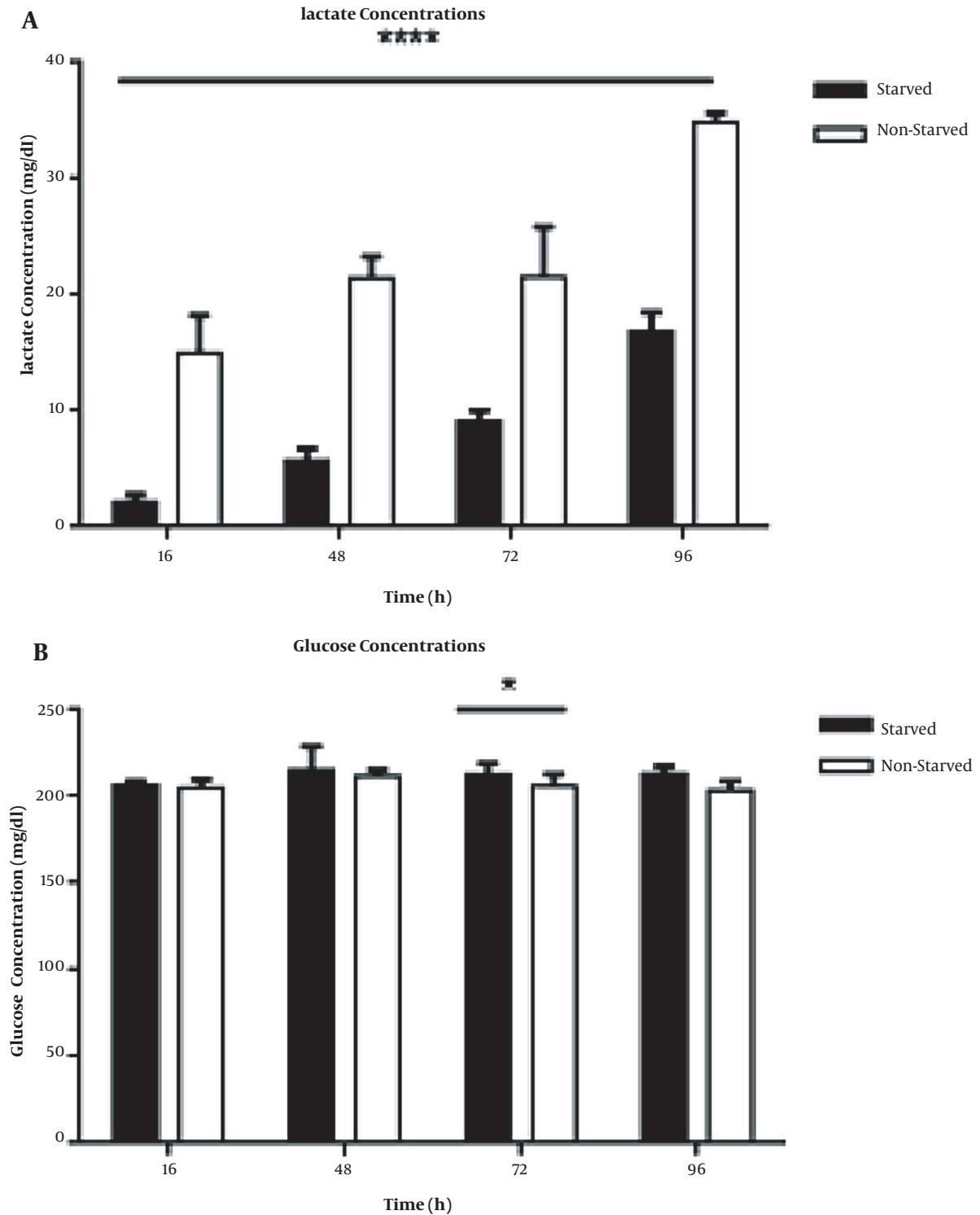


Figure 2. The levels of lactate and glucose in starved and non-starved PBMCs culture supernatants (n = 9; three samples with triplicate wells for each time point). A, The lactate levels were significantly lower in starved PBMCs than in non-starved controls ($P < 0.0001$) for all time points. B, The levels of glucose in starved and non-starved PBMCs culture supernatants (n = 9; three samples with triplicate wells for each time point). At time point 72 h, the difference in glucose levels between starved and non-starved groups was significant ($P < 0.05$). The results are shown as mean \pm SD. Error bars show SD; * indicates $P < 0.05$, ** indicates $P < 0.01$, and *** shows $P < 0.001$; $P < 0.05$ was considered as the statistically significant level.

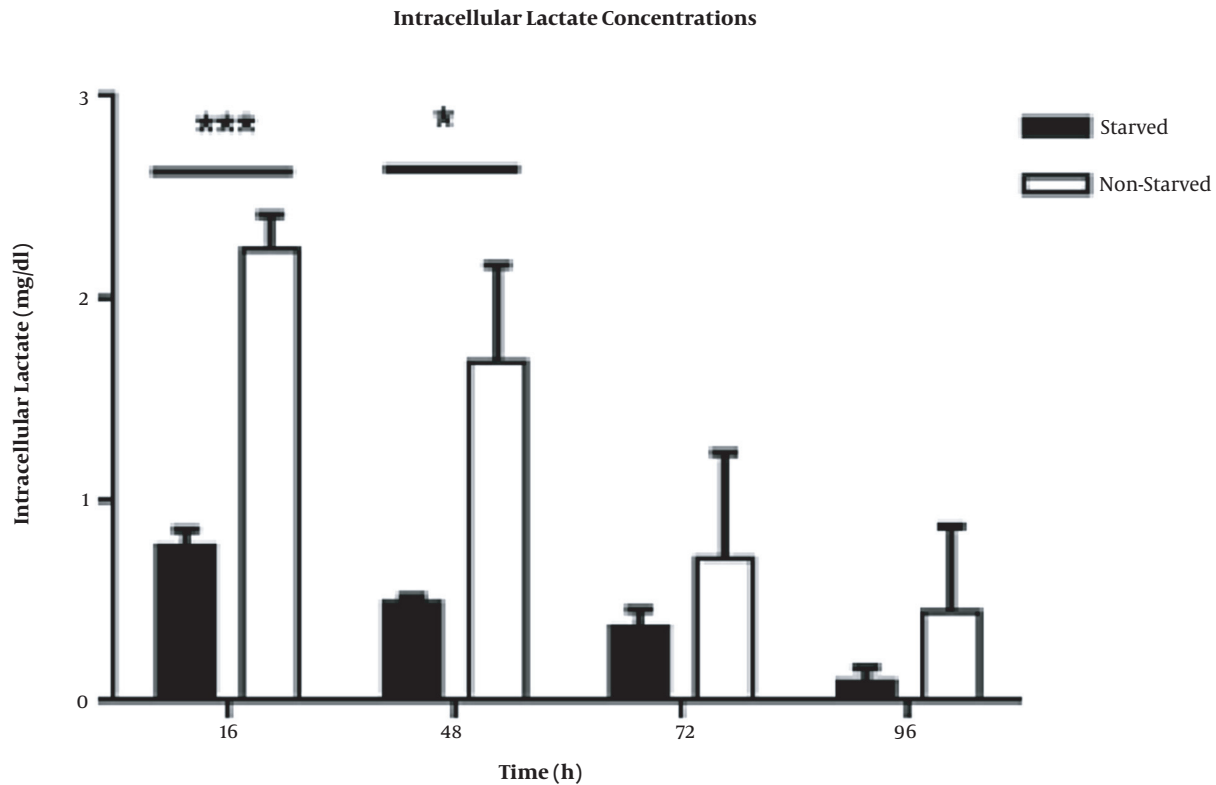


Figure 3. Intracellular lactate levels in starved and non-starved PBMCs. The concentrations of lactate significantly decreased in starved immune cells, especially at time point 16 h ($P < 0.0001$). This decrement was also significant at time point 48 h ($P < 0.05$). The data were presented as mean \pm SD ($n = 4$). Error bars show SD. * indicates $P < 0.05$ and *** indicates $P < 0.0001$; $P < 0.05$ was the statistically significant level.

reduction analysis. The MTT reduction is considered an indicator of mitochondrial function (17). This water-soluble dye can be converted to water-insoluble crystals by mitochondrial dehydrogenase, especially succinate dehydrogenase (18). Interestingly, at single-cell levels, we repeatedly observed that compared to non-starved controls, in the starved PBMCs population, there were fewer macrophage-like cells with lower levels of purple crystals, indicating the lower activity of cellular mitochondria in such cells. In both groups, lymphocytes were almost free of purple crystals; thus, the lower OD values obtained in the MTT assay could be attributed to the enzymatic activity of spindle shape macrophage-like cells. Moreover, MTT reduction by cells represents the activity of the electron transport chain (17), which is coupled to lactate production, the end product of the glycolysis pathway that occurs in the cytoplasm. In line with this observation, we found that starved PBMCs exhibited a lower level of lactate at both extra and intra-

cellular levels, implying that the reduced levels of glycolysis in starved PBMCs resulted in dampening in electron transport activity of mitochondria and consequently led to decreased levels of MTT reduction. To interpret these findings, we hypothesized that serum starvation triggered the ISR in PBMCs and subsequently led to the downregulation of general protein production, including enzymes involved in glycolysis and electron transport chain. Prolonged ISR could lead to cell death induction after 72 h decreasing the cell number, which, in turn, enhanced the discrepancy in lactate production between starved and non-starved cells. Further study is required to examine this hypothesis. In contrast to these obvious alterations in lactate concentration, we did not find remarkable changes in glucose levels between the two groups, except at the time point of 72 h ($P < 0.05$). This lack of harmony between glucose consumption and lactate production may originate from the light absorption-based method we used for glu-

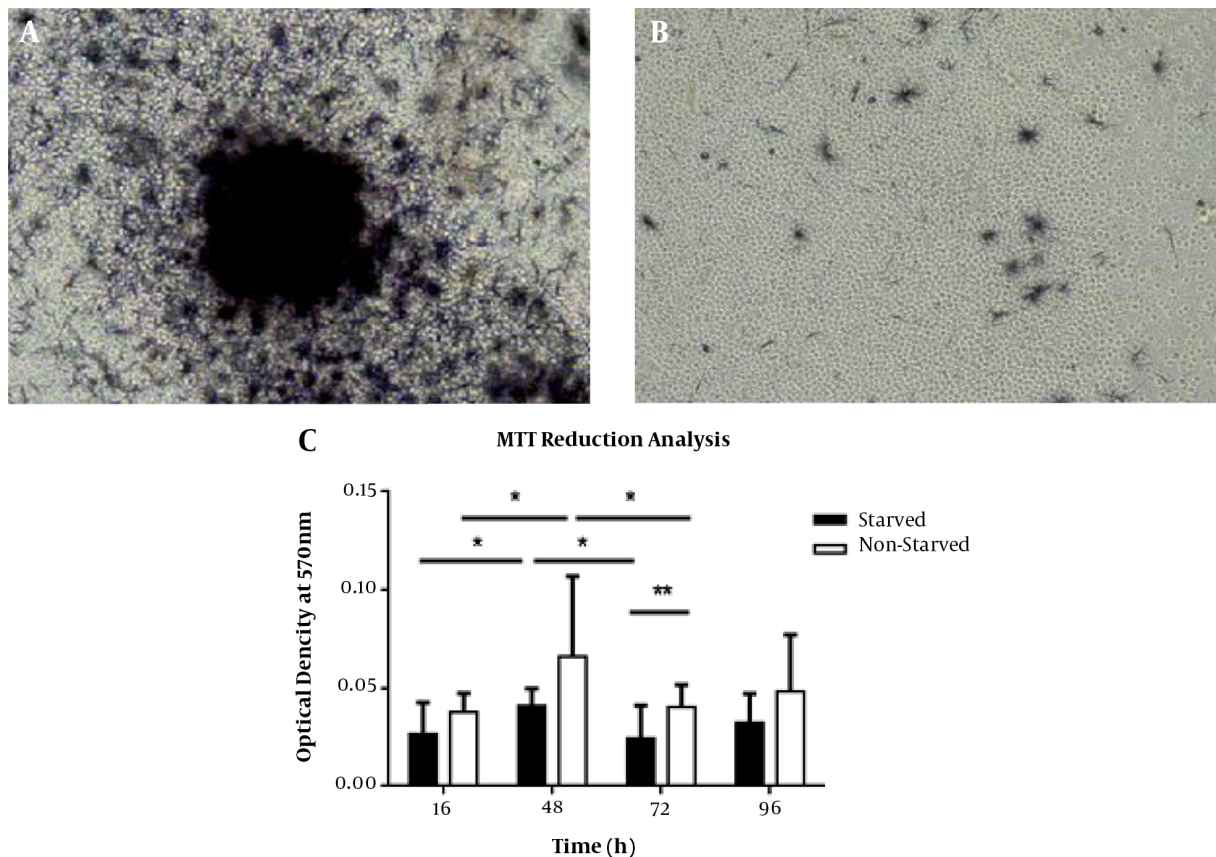


Figure 4. Qualitative and quantitative evaluation of MTT reduction capacities in starved and non-starved PBMCs. All starved and non-starved PBMCs were re-fed by fresh RPMI + 10% FBS for 96 h. A, 48 h cultured PBMCs, as control cells, intensively formed formazan crystals. B, Decreased levels of MTT reduction in 48 h starved PBMCs. C, There was a significant difference between starved and non-starved PBMCs in MTT reduction after 72 h of cell incubation ($P < 0.01$). Moreover, there were remarkable alterations in the activity of MTT reduction in both groups. The highest levels of MTT reduction occurred in 48 h cultured cells for both groups. Results are presented as mean \pm SD ($n=3$). Error bars show SD. * indicates $P < 0.05$ and *** shows $P < 0.0001$. $P < 0.05$ was considered as the statistically significant level.

cose detection in cell culture supernatant instead of fluorescent emission-based techniques used by other groups for the same purpose (19).

Collectively, the importance of these findings becomes clear when we take into account the monocytes/macrophages, which are the main cellular components in innate immunity and respond to a variety of substances, from “self” originated molecules released from damaged tissue (damage-associated molecular pattern, DAMP) to “non-self” molecules derived from different pathogenic germs from viruses and bacteria to fungi (pathogen-associated molecular pattern, PAMP). Both DAMP and PAMP trigger danger signals into the cells through Pattern Recognition Receptors (PRR), which, in turn, enhances inflammatory cytokine release via multi-component inflammasomes. Macrophages are also

activated by type 1 T helper cells (Th1). Hyperactivation of macrophages is the main culprit in autoinflammatory diseases like multiple sclerosis, as well as the newly emerged viral disease, the COVID-19 pandemic. However, activation of macrophages requires metabolic reprogramming, which results in elevated levels of oxidative phosphorylation in mitochondria. Also, Th1 cells need such reprogramming. Thus, those activated cells are vulnerable to metabolic stress compared to non-activated cells. In recent years, this weakness of activated immune cells formed the core of a therapeutic strategy emphasizing the targeting of immune cells metabolism for the treatment of some autoinflammatory diseases like multiple sclerosis by some drugs such as metformin and dimethyl fumarate. The latter drug is able to skew M1 inflammatory type macrophages to M2 anti-inflammatory

macrophages. Moreover, this drug can shift proinflammatory Th1 to anti-inflammatory Th2 type cells. Further clinical trial studies are required to evaluate this presumption. We have already reported that serum starvation can be used as an immunomodulator tool by increasing CD4+CD25+FOXP3+CD127-T-regulatory cells (16). Moreover, in the mouse model, we recently showed that starved bone marrow cell transplantation alleviated the acute graft versus host disease manifestation (under review manuscript). The latter finding shows that autologous starved immune cells therapy may have some benefits for the treatment of autoinflammatory diseases like multiple sclerosis, which dimethyl fumarate is currently administered for this disease. Taken together, this study showed that under serum starvation stress, lactate production is reduced in PBMCs, and total oxidative mitochondrial activity is diminished in macrophage-like cells. These findings open a new window in targeting immune cell metabolism through drugs such as dimethyl fumarate for the treatment of hyperinflammation-mediated diseases like COVID-19 or using autologous starved immune cell therapy to modulate adverse reactions of autoinflammatory diseases, including multiple sclerosis.

Acknowledgments

This study was financially supported by the Student Research Committee of Babol University of Medical Sciences.

Footnotes

Authors' Contribution: The manuscript has been read and approved by all authors.

Conflict of Interests: The authors declare that there is no conflict of interest.

Ethical Approval: IR.MUBABOL.HRI.REC.1397.321.

Funding/Support: This study was financially supported by the Student Research Committee of Babol University of Medical Sciences.

Informed Consent: Patient consented to participate in the study.

References

- Jacobs SR, Herman CE, Maciver NJ, Wofford JA, Wieman HL, Hammen JJ, et al. Glucose uptake is limiting in T cell activation and requires CD28-mediated Akt-dependent and independent pathways. *J Immunol.* 2008;**180**(7):4476–86. doi: [10.4049/jimmunol.180.7.4476](#). [PubMed: [18354169](#)]. [PubMed Central: [PMC2593791](#)].
- Cho H, Hur HW, Kim SW, Kim SH, Kim JH, Kim YT, et al. Pre-treatment neutrophil to lymphocyte ratio is elevated in epithelial ovarian cancer and predicts survival after treatment. *Cancer Immunol Immunother.* 2009;**58**(1):15–23. doi: [10.1007/s00262-008-0516-3](#). [PubMed: [18414853](#)].
- Romero-Garcia S, Moreno-Altamirano MM, Prado-Garcia H, Sanchez-Garcia FJ. Lactate contribution to the tumor microenvironment: Mechanisms, effects on immune cells and therapeutic relevance. *Front Immunol.* 2016;**7**:52. doi: [10.3389/fimmu.2016.00052](#). [PubMed: [26909082](#)]. [PubMed Central: [PMC4754406](#)].
- Warburg O, Wind F, Negelein E. The metabolism of tumors in the body. *J Gen Physiol.* 1927;**8**(6):519–30. doi: [10.1085/jgp.8.6.519](#). [PubMed: [19872213](#)]. [PubMed Central: [PMC2140820](#)].
- Stepanenko AA, Dmitrenko VV. Pitfalls of the MTT assay: Direct and off-target effects of inhibitors can result in over/underestimation of cell viability. *Gene.* 2015;**574**(2):193–203. doi: [10.1016/j.gene.2015.08.009](#). [PubMed: [26260013](#)].
- Pakos-Zebrucka K, Koryga I, Mnich K, Lujic M, Samali A, Gorman AM. The integrated stress response. *EMBO Rep.* 2016;**17**(10):1374–95. doi: [10.15252/embr.201642195](#). [PubMed: [27629041](#)]. [PubMed Central: [PMCS048378](#)].
- Weichhart T. Mammalian target of rapamycin: a signaling kinase for every aspect of cellular life. *Methods Mol Biol.* 2012;**821**:1–14. doi: [10.1007/978-1-61779-430-8_1](#). [PubMed: [2215056](#)].
- Carroll B, Korolchuk VI, Sarkar S. Amino acids and autophagy: cross-talk and co-operation to control cellular homeostasis. *Amino Acids.* 2015;**47**(10):2065–88. doi: [10.1007/s00726-014-1775-2](#). [PubMed: [24965527](#)].
- Cao C, Subhawong T, Albert JM, Kim KW, Geng L, Sekhar KR, et al. Inhibition of mammalian target of rapamycin or apoptotic pathway induces autophagy and radiosensitizes PTEN null prostate cancer cells. *Cancer Res.* 2006;**66**(20):10040–7. doi: [10.1158/0008-5472.CAN-06-0802](#). [PubMed: [17047067](#)].
- Pirkmajer S, Chibalin AV. Serum starvation: caveat emptor. *Am J Physiol Cell Physiol.* 2011;**301**(2):C272–9. doi: [10.1152/ajpcell.00091.2011](#). [PubMed: [21613612](#)].
- Taylor CT, Colgan SP. Regulation of immunity and inflammation by hypoxia in immunological niches. *Nat Rev Immunol.* 2017;**17**(12):774–85. doi: [10.1038/nri.2017.103](#). [PubMed: [28972206](#)]. [PubMed Central: [PMCS799081](#)].
- Mehta P, McAuley DF, Brown M, Sanchez E, Tattersall RS, Manson JJ, et al. COVID-19: consider cytokine storm syndromes and immunosuppression. *Lancet.* 2020;**395**(10229):1033–4. doi: [10.1016/S0140-6736\(20\)30628-0](#). [PubMed: [32192578](#)]. [PubMed Central: [PMC7270045](#)].
- Golpour M, Fattahi S, Niaki HA, Hadipoor A, Abedian Z, Ahangarian GR, et al. Starved human fibroblasts secrete acidic proteins inducing post re-feeding proliferation and in vitro cell migration: a potential tool for wound healing. *Biol Cell.* 2014;**106**(5):139–50. doi: [10.1111/boc.201300063](#). [PubMed: [24612410](#)].
- Pourbagher R, Akhavan-Niaki H, Jorsaraei SGA, Fattahi S, Sabour D, Zabihi E, et al. Targeting LA7 breast cancer stem cells of rat through repressing the genes of stemness-related transcription factors using three different biological fluids. *Gene.* 2020;**734**. doi: [10.1016/j.gene.2020.144381](#).
- Rahmani M, Khorasani HR, Golpour M, Shabestani Monfared A, Nat-taj H, Abedian S, et al. Stable down-regulation of HLA class-I by serum starvation in human PBMCs. *Iran J Immunol.* 2016;**13**(1):54–63. [PubMed: [27026047](#)].

16. Rahmani M, Mohammadnia-Afrouzi M, Nouri HR, Fattahi S, Akhavan-Niaki H, Mostafazadeh A. Human PBMCs fight or flight response to starvation stress: Increased T-reg, FOXP3, and TGF-beta1 with decreased miR-21 and Constant miR-181c levels. *Biomed Pharmacother*. 2018;**108**:1404–11. doi: [10.1016/j.biopha.2018.09.163](https://doi.org/10.1016/j.biopha.2018.09.163). [PubMed: [30453448](https://pubmed.ncbi.nlm.nih.gov/30453448/)].
17. Ross KL, Eisenstein RS. Iron deficiency decreases mitochondrial aconitase abundance and citrate concentration without affecting tricarboxylic acid cycle capacity in rat liver. *J Nutr*. 2002;**132**(4):643–51. doi: [10.1093/jn/132.4.643](https://doi.org/10.1093/jn/132.4.643). [PubMed: [11925455](https://pubmed.ncbi.nlm.nih.gov/11925455/)].
18. Rai Y, Pathak R, Kumari N, Sah DK, Pandey S, Kalra N, et al. Mitochondrial biogenesis and metabolic hyperactivation limits the application of MTT assay in the estimation of radiation induced growth inhibition. *Sci Rep*. 2018;**8**(1):1531. doi: [10.1038/s41598-018-19930-w](https://doi.org/10.1038/s41598-018-19930-w). [PubMed: [29367754](https://pubmed.ncbi.nlm.nih.gov/29367754/)]. [PubMed Central: [PMC5784148](https://pubmed.ncbi.nlm.nih.gov/PMC5784148/)].
19. Yamamoto N, Ueda-Wakagi M, Sato T, Kawasaki K, Sawada K, Kawabata K, et al. Measurement of glucose uptake in cultured cells. *Curr Protoc Pharmacol*. 2015;**71**:12.14.1–12.14.26. doi: [10.1002/0471141755.ph1214s71](https://doi.org/10.1002/0471141755.ph1214s71). [PubMed: [26646194](https://pubmed.ncbi.nlm.nih.gov/26646194/)].